PHYSICAL REVIEW C VOLUME 16, NUMBER 6 DECEMBER 1977

Statistical model radiation widths for $75 < A < 130$ and the enhancement of P-wave neutron capture for $A \approx 90$*

C. H. Johnson
Oak Ridge National Laboratory, Oak Ridge, Tennessee 37830
(Received 11 July 1977)

Statistical model calculations of radiation widths are made on the basis of the Axel-Brink hypothesis with two free parameters for the normalization and A dependence of the low-energy tail of the giant electric dipole resonance. The two parameters are adjusted to fit known radiation widths with a standard deviation of about ±25% for s-wave neutron resonance levels in nuclei with $75 < A < 130$. The resulting $E1$ strength functions are consistent with known values over a large mass region for transitions to low-lying states. The $M1$ transitions are included. The level densities or nuclear temperatures for the analysis are deduced by fitting the backshifted Fermi-gas model to the total number of states near the ground state and to the s-wave spacings at neutron binding. The low density of levels for $A \approx 90$ gives rise to statistical enhancement of p-wave relative to s-wave neutron radiative capture. The sum of calculated radiation widths for p-wave resonances plus calculated radiation widths for p-wave valency capture agree well with published experimental values.

[NUCLEAR REACTIONS Calculated $\langle \Gamma_\gamma \rangle$, $75 < A < 130$.]

I. INTRODUCTION

In neutron capture the dominant radiative transitions occur statistically with no correlation with the details of the initial state or the manner in which it was formed. Many data are available on radiation widths for decay from the states formed by neutron capture. The aim here is to describe observed average radiation widths by the statistical model. The chosen mass region, $75 < A < 130$, is a small part of the Periodic Table but is large enough to give nontrivial parameters. Also it includes a region near $A = 90$ which is of special interest, as discussed below. Such a study is important not only for evaluating the role of statistical processes but also for practical applications to (n,γ), (p,γ), and other reactions. Yet there is a dearth of such studies in the journals. Perhaps that is because there must be several assumptions and the data needed for the parameters in these assumptions are often fragmentary. Involved are a basic assumption that all final states have the same energy-dependent γ-ray strength, the form of that strength, its parameters for each nucleus, and the relative $E1$ and $M1$ strengths. Also involved are the assumed form of the level density function, its parameters for each nucleus, and the details (J^π and energy) of the low-lying final states which are not described by a continuous function. An ideal treatment of each of the foregoing items would be exhaustive. The present treatment states the assumptions, deduces the parameters from available data, and combines all into a useful whole. In the process two free parameters are adjusted to fit the average total radiation widths for $75 < A < 130$, and the resulting parameters are found to be consistent with the rather limited data available on partial widths for a broader mass region. Throughout, approximations are tentatively introduced to illustrate the essentials that might otherwise be buried in the details. The role of nuclear temperature is particularly emphasized.

An important reason for this study is to better understand the interesting nonstatistical effects that may occur.[1-4] The valency model[1,2] introduces an amplitude proportional to $\theta_\lambda \theta_f$, i.e., the product of the neutron dimensionless reduced widths in the initial and final states λ and f. If valency capture occurs, the partial radiation width $\Gamma_{\lambda f}$ is correlated to $\theta_\lambda^2 \theta_f^2$, and the total radiation width Γ_λ may have a large entrance-channel correlation coefficient $\rho(\theta_\lambda^2, \Gamma_\lambda)$. Near $A = 90$, in particular, $E1$ valency transitions can occur from initial states having relatively large $3p$ components to low-lying final states having large contributions from the $3s$ and $2d$ orbits, which follow closure of the 50-neutron shell.

Other amplitudes proportional either to θ_λ or to θ_f may be present.[3,4] In fact, the early evidence for nonstatistical transitions in this mass region was found[5,6] from four p-wave resonances in ^{93}Nb(n,γ) which showed correlations to final but not initial states. These were interpreted as par-

ticle-hole annihilations.[5,6]

In the first observations[7,8] of valency capture in this mass region three of the four p-wave resonances for neutron energies below 1 keV in ^{98}Mo(n,γ) showed significant enhancements for transitions to low-lying final states. Later data[9] up to 5.3 keV showed only the two resonances at 429 and 612 eV to be correlated to $\theta_\lambda^2\theta_f^2$ and two or three of the remaining 15 correlated to θ_f^2. Further measurements[10] up to 15 keV of the total radiation widths for p-wave neutrons, $\Gamma_{\lambda p}$, showed the average initial-state correlations to be quite small.

More pronounced valency transitions or entrance-channel correlations were found in the immediate vicinity of the 50-neutron shell ($A \approx 90$). Early low-energy data[8] for ^{92}Mo(n,γ) indicated valency transitions to two final states having large $d_{5/2}$ and $d_{3/2}$ components. Although later high resolution data over a wider energy range[11] confirmed the valency transitions only to the $d_{3/2}$ state, the $\Gamma_{\lambda p}$ for resonances up to 50 keV showed[10] significant entrance-channel correlations. Entrance-channel correlations for $\Gamma_{\lambda p}$ have been observed[12-16] also for ^{88}Sr, ^{89}Y, and ^{90,91,92,94}Zr. For ^{90}Zr, earlier measurements[17] on the inverse ^{91}Zr(γ,n) reaction showed correlations for ground state transitions to levels corresponding to p-wave neutron resonances below 225 keV.

The valency transitions enhance the average $\langle\Gamma_\lambda\rangle_p$ but not the s-wave average $\langle\Gamma_\lambda\rangle_s$, for which no valency transitions are expected in this mass region. For $88 \leq A \leq 100$ Musgrove *et al.*[10,16] and Boldeman *et al.*[12-15] observed enhancements ranging systematically, except for odd-even effects, from a maximum for ^{88}Sr to a negligible value for ^{100}Mo. For all but ^{94}Zr the enhancements were larger than the authors predicted on the basis of the valency model[1,2] from known θ_λ^2 and θ_f^2. Although the observed and predicted enhancements were consistent within the uncertainties in about half of the cases, the observed values were significantly larger than predicted for ^{90}Zr and ^{92,94,96,98}Mo. The authors concluded that other nonstatistical effects must be present, probably doorway transitions to the single-particle final states.

A major point of the present paper is that such conclusions cannot be made on that basis; the excess p-wave widths beyond the valency predictions are expected from the statistical model simply because the $E1$ dipole strengths are larger than $M1$ and the low-lying states near $A = 90$ are mostly even parity. The excess is particularly large near $A = 90$ because the level densities at neutron binding are small; thus, the partial widths for transitions to given low-lying final states are distributed among fewer resonant states.

II. γ-RAY STRENGTH FUNCTION

The partial width for electric dipole radiation of energy E_γ from initial states λ of given J^π at excitation E_x, averaged over λ, to a final state f at $E_x - E_\gamma$ is given by[18]

$$\langle\Gamma_{\lambda f}\rangle_J = S_{E1}(E_\gamma)E_\gamma{}^3/\rho_J(E_x), \tag{1}$$

where $\rho_J(E_x)$ is the density of levels with spin J and given parity, even or odd, and $S_{E1}(E_\gamma)$ is the $E1$ strength function. The final state must satisfy the dipole selection rules. Implicit is the basic Axel-Brink hypothesis[19,20] that each final state f has built upon it the same giant dipole resonance (GDR) as does the ground state. Rosenzweig[21] has justified this assumption in terms of a hydrodynamic model. Thus $S_{E1}(E_\gamma)$ is assumed to be a function only of the γ-ray energy.

A less fundamental assumption of the Axel-Brink hypothesis is that the classical Lorentz form that describes the GDR for photon energies well above the photoneutron threshold can be extrapolated down to the low energies of the capture radiations. If that were strictly valid the strength functions could be deduced at once from the observed[22] photonuclear resonances by use of the expression[18]

$$S_{E1}(E_\gamma) = \tfrac{1}{3}(2.6\times10^{-7})\frac{\sigma_g\Gamma_g{}^2E_\gamma}{(E_g{}^2-E_\gamma{}^2)^2+\Gamma_g{}^2E_\gamma{}^2}, \tag{2}$$

where E_g and Γ_g are the GDR energy and width in MeV and σ_g is the peak cross section in mb. The strength is in MeV^{-3}. The observed[22] E_g in the present mass region are about 16 MeV and well described by

$$E_g = 76/A^{1/3}\ \text{MeV}. \tag{3}$$

The integrated cross sections are consistent with the electric dipole sum rule, which in the absence of exchange forces can be written[23]

$$\Gamma_g\sigma_g = 40\pi\frac{e^2\hbar}{Mc}\frac{NZ}{A}$$
$$= 38NZ/A\ \text{MeV mb}. \tag{4}$$

However the extrapolation to lower energies is not expected to be reliable because the Lorentzian does not describe the GDR exactly and because only about 1% of the dipole sum is distributed below $E_\gamma \approx 8$ MeV. Also deviations such as the "pigmy" resonance[18] may be present. Nevertheless, since neutron capture spectra have shown that the energy dependence of the Lorentzian tail is about right and certainly better than a constant strength function, a reasonable procedure is to retain the Lorentzian form but to parametrize it in order to describe average radiation widths. The parametrization could be formulated in various ways. My procedure is to retain Eqs. (3,4) for E_g and

$\sigma_g\Gamma_g$ but to introduce a function for Γ_g, namely

$$\Gamma_g = 88A/NZ \text{ MeV}. \quad (5)$$

Although this function is presented here for the sake of completeness of this section, its justification is deferred to Sec. IV, where its choice in conjunction with the level densities of Sec. III is shown to give good fits to the average radiation widths for s-wave resonances for $75<A<130$. Essentially the parametrization is designed to describe the multitude of low-energy radiations to high-lying states but, as shown in Sec. VII, it also leads to strength functions consistent with published values for energetic primary transitions to lower states. As discussed in Sec. V and the Appendix, different parameters would be required if the density function were changed.

The resulting σ_g and Γ_g, so chosen to fit observed radiation widths and to satisfy the sum rule limit, generally disagree with the observed[22] σ_g and Γ_g. The essential disagreements can be illustrated by an approximation to the strength; since the average capture γ-ray energies are much less than E_g, typically $E_g/5$, we have approximately

$$S_{E1}(E_\gamma) \propto (\sigma_g\Gamma_g^2/E_g^4)E_\gamma. \quad (6)$$

Substituting from Eqs. (4) and (5) we find the coefficient of E_γ;

$$\sigma_g\Gamma_g^2/E_g^4 = cA^{4/3}, \quad (7)$$

where c is a given constant. The quantity $\sigma_g\Gamma_g^2/E_g^4$ is plotted in Fig. 1 along with points deduced from the observed[22] GDR. We see that the empirical curve for fitting the radiation widths deviates considerably from the extrapolated GDR except near $A=90$. Basically the use of the curve constitutes an analysis with two free parameters corresponding to the magnitude and slope of the curve.

Small corrections must be made for $M1$ transitions. Here the Axel-Brink hypothesis is assumed also for $M1$ radiation. From average-resonance capture measurements Bollinger[24] and his co-workers found the average $E1/M1$ ratios to be remarkably constant, 7 ± 1, over the mass region of their work, about $A=105$ to 240. Although this constant is not valid for light nuclei it can reasonably be extrapolated from $A=105$ to 75 for use in the present analysis. The energy dependences for the $M1$ strengths are poorly known but are not critical because the $M1/E1$ ratio is small. Bollinger and Thomas[25] found evidence in ^{106}Pd for an $M1$ giant-resonance peak near 7.8 MeV but, in general, Bollinger[24] concluded that the $E1$ and $M1$ energy dependences for capture radiations are about the same. Even for ^{106}Pd the dependences are similar below the 7.8-MeV peak. Therefore, I assume the

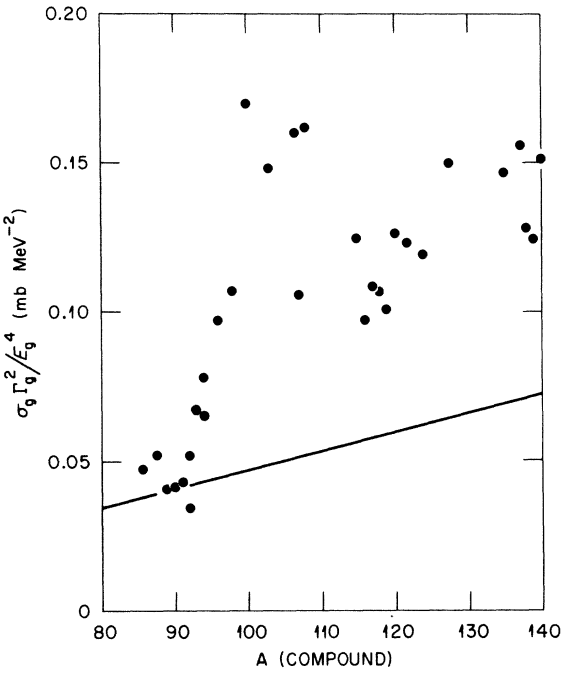

FIG. 1. Experimental values of the combined Lorentzian factor, $\sigma_g\Gamma_g^2/E_g^4$, from Berman's (Ref. 22) tabulation of $E1$ giant dipole resonance parameters. The curve shows values assumed in order to fit radiation widths for the present analysis, where E_g, σ_g, and Γ_g are given by Eqs. (3), (4), and (5). The abscissa indicates that the parameters apply to neutron-capture compound nuclei.

$M1$ dependence is approximated by the $E1$ dependence;

$$S_{M1}(E_\gamma) = S_{E1}(E_\gamma)/7. \quad (8)$$

This assumption for the capture radiations *does not* imply that the $M1$ maximum actually occurs at the same place as the $E1$ maximum near 16 MeV.

In summary, the strength functions for the following analysis are defined by Eqs. (2)–(5) and (8).

III. LEVEL DENSITIES

The total dipole radiation width averaged over states of J^π at E_x can be expressed as the sum of two terms;

$$\langle\Gamma_\lambda\rangle_{J\pi} = \Gamma_{dJ\pi} + \Gamma_{cJ}, \quad (9)$$

where $\Gamma_{dJ\pi}$ is the sum over the "discrete" states below E_c, all having known I^π, and Γ_{cJ} is an integral over the closely spaced "continuum" of states from E_c to E_x.

For the discrete states,

$$\Gamma_{dJ\pi} = \left[\sum_{fE1} S_{E1}(E_\gamma)E_\gamma^3 + \sum_{fM1} S_{M1}(E_\gamma)E_\gamma^3\right]/\rho_{J\pi}(E_x), \quad (10)$$

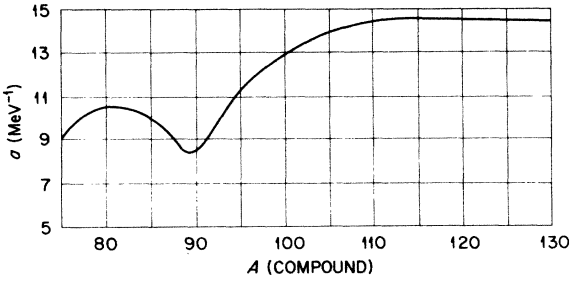

FIG. 2. Assumed A dependence of the Fermi-gas constant a based on the empirical evaluations in Refs. 29 and 30.

where $E_\gamma = E_x - E_f$ for each final state f and the summation subscripts $fE1$ and $fM1$ indicate final states that satisfy the selection rules. Although the level density $\rho_J(E)$ is assumed to be independent of parity, the π subscript is included as a reminder that the selection rules apply to a definite initial J^π.

For the "continuum" states

$$\Gamma_{cJ} = \int_0^{E_x - E_c} S(E_\gamma) E_\gamma^3 \sum_{I=J-1}^{I=J+1} \rho_I(E_x - E_\gamma) dE_\gamma / \rho_J(E_x), \tag{11}$$

where $S(E_\gamma) \equiv S_{E1}(E_\gamma) + S_{M1}(E_\gamma)$. This term is independent of parity because the final states include equally both parities; it depends on the sum $S(E_\gamma)$ rather than on the $E1/M1$ ratio.

The literature[26] includes many studies of the energy and J dependence of level densities. For levels of given J and parity, odd or even,

$$\rho_J(U) = \rho(U)(J+\tfrac{1}{2})(2\sigma^2)^{-1} \exp[-(J+\tfrac{1}{2})^2/2\sigma^2], \tag{12}$$

where σ^2 is a spin cutoff factor and $\rho(U)$ is the total density for all J and both parities at an effective excitation energy U. The pairing energy is accounted for by measuring U from a fictive ground state Δ; $U = E - \Delta$ where E is the actual excitation energy.

The Fermi-gas model is used here. Of two expressions often used for the model, the following gives[27] the slightly less accurate description of a two-fermion gas with equidistant nucleon spacings, but it is simpler for computations:

$$\rho(U) = \frac{\exp[2\sqrt{aU}]}{12\sqrt{2}\, a^{1/4} U^{5/4} \sigma}, \tag{13}$$

where a is the gas constant. The expression for σ^2 used below is from Gilbert and Cameron[28] and corresponds to about 75% of the rigid body moment of inertia:

$$\sigma^2 = 0.0888(aU)^{1/2} A^{2/3}. \tag{14}$$

In recent studies[26,29,30] both a and Δ have been treated as free parameters for fitting observed level densities. This is called the "back-shifted" model because the fictive ground state is generally below the conventional pairing energy.[28] A common procedure[29,30] for determining the mass dependence of a and Δ is to fit two data for each nucleus, namely the total number of states observed in some interval near the ground state and the spacing of s-wave neutron resonances at the separation energy. A slight modification of that procedure is used for most of the present analysis in that the smooth empirical curve in Fig. 2 is assumed for a. I drew the curve visually to fit values deduced empirically by Dilg *et al.*[29] (for σ^2 corresponding to 75% of the rigid body moment of inertia) and by Holmes *et al.*[30]

With a given, I deduced the Δ's in Table I by fitting $\int \rho(U)dU$ to the total number of levels in selected energy regions near the ground states of the adopted level schemes in the Nuclear Data Sheets,[31] supplemented by a few recent references.[6,9,32] The selection of these samples of "total density" is somewhat subjective because each sample should be from an energy region far enough above the ground state to be representative of the "continuum" and yet low enough to ensure that few levels have been missed. The region must begin above Δ to avoid the singularity in $\rho(U)$ and should be above the nonphysical minimum in $\rho(U)$. On the average I chose samples with 24 levels beginning 0.7 MeV above Δ. Actually, Δ is not too critical for predicting Γ_{cJ} even though it is critical for level densities. A change in Δ corresponding to 10% of U_x, a rather large change, would alter the densities at neutron binding by a factor of 2 but would alter Γ_{cJ} only ~20%. On the other hand, since the discrete term varies directly with the level spacings, it is sensitive to Δ as well as to a.

The validity of the smooth curve for a and of the selection of total densities can be judged by comparing the predicted and observed s-wave resonance spacings listed in Table I. The related back-shifted neutron separation energies, U_n, are also listed. The observed spacings are from the tabulation of Dilg *et al.*[29] and from the more recent data[10,12-16] for $88 \leq A \leq 100$. Generally the agreement is within the experimental uncertainties of measuring $\langle D \rangle_s$ and deducing Δ. Of course, the agreement to about ±30% with Dilg's tabulation is not surprising since those data were used originally to deduce the smooth curve for a. Nevertheless, it shows that a smooth curve is valid for most nuclei. Furthermore, the fits to the more recent spacings for $91 \leq A \leq 100$ are predictions because many of the values available to Dilg had mixtures of s and p waves.

We might expect the predicted spacings to be

TABLE I. Level density parameters: back-shifted energy Δ, U at neutron binding energy, calculated and observed average s-wave neutron resonance spacings, lower limit E_c for integrating Γ_{cJ}.

Target	Δ (MeV)	U_n (MeV)	Calc. $\langle D\rangle_s$ (eV)	Exp.[a] $\langle D\rangle_s$ (eV)	E_c (MeV)
^{77}Se	1.10	9.4	95	120	1.75
^{78}Se	0.70	6.28	2 880	1 000	1.00
^{79}Br	−1.25	9.13	57	60	0.25
^{85}Rb	−0.4	9.05	91	>130	1.20
^{88}Sr	1.2	5.30[b]	30 000[b]	48 000[c]	2.70
^{89}Y	0.3	6.56	4 400	2 200[c,d]	1.70
^{90}Zr	0.35	6.90[e]	5 200[e]	8 600[c]	2.15
^{91}Zr	1.6	7.04	650	640[c]	2.00
^{92}Zr	0.6	6.16	4 000	4 000[c]	1.44
^{92}Mo	1.0	7.07	1 710	2 400[c]	2.00
^{93}Nb	−0.9	8.13	91	64	1.35
^{94}Zr	1.2	5.28	5 432	4 500[c]	1.90
^{94}Mo	0.7	6.68	1 260	1 150[c]	1.90
^{95}Mo	1.35	7.80	67	80[c]	2.30
^{96}Mo	0.4	6.42	988	950[c]	1.15
^{97}Mo	0.95	7.69	46	42[c]	1.80
^{98}Mo	−0.1	6.03	1 055	950[c]	1.16
^{99}Ru	1.5	8.17	29	34[c]	1.70
^{100}Mo	−1.2[f]	6.59	420[f]	420[c]	0.50
^{101}Ru	1.35	7.87	19	18	1.50
^{103}Rh	−1.3	8.30	25	27	0.15
^{105}Pd	1.15	8.46	7	9	1.90
^{107}Ag	−0.7	7.97	23	23	0.19
^{109}Ag	−1.1	7.90	23	18	0.10
^{110}Cd	0.15	6.83	147		0.50
^{111}Cd	1.45	7.95	21	26	1.80
^{112}Cd	−0.15	6.69	176	198	0.20
^{113}Cd	1.55	7.49	36	25	1.80
^{113}In	−0.3	7.61	11	11	0.30
^{115}In	−0.7	7.48	13	10.7	0.30
^{117}Sn	1.7	7.63	32	45	2.10
^{121}Sb	−1.0	7.81	11	12.5	0.10
^{123}Sb	−1.0	7.47	15	25	0.01
^{123}Te	1.2	8.22	17	26	2.00
^{124}Te	−0.5	7.08	130	147	0.50
^{125}Te	1.35	7.76	31	38	1.60
^{126}Te	−0.15	6.44	280	207	0.05
^{128}Te	0.0	6.09	440	262	0.1
^{129}Xe	1.1	8.15	21	35	1.6

[a] Spacings not noted otherwise are from Dilg *et al.* (Ref. 29).
[b] Calculated for 140-keV neutrons.
[c] AAECRE-ORELA (Refs. 10 and 12–16).
[d] Recently Camarda (Ref. 33) found $\langle D\rangle_s = 4.0$ keV.
[e] Calculated for 50-keV neutrons.
[f] The shift Δ chosen to fit $\langle D\rangle_s$.

least reliable in the critical region very near mass 90. Indeed, the table shows large discrepancies for the 50-neutron nuclei, ^{88}Sr, ^{89}Y, and ^{90}Zr. However, those experimental values could have large errors because of the poor statistics inherent in large spacings. In fact, Camarda[33] recently found a spacing for ^{89}Y of 4.0 keV in agreement with the prediction but almost a factor of 2 larger than the listed measurement.

Further comments on level densities are given in Sec. V and in the Appendix.

IV. s-WAVE WIDTHS FOR $75 < A < 130$

Assuming the strength functions from Sec. II and the density parameters from Fig. 2 and Table I, I calculated radiation widths by numerical integration of Eqs. (10) and (11) using a subroutine from a general Hauser-Feshbach program HELGA written by Penny.[34] (The routine integrates the exponential terms accurately for each ΔE of the numerical integration.) Table I includes the boundary energies E_c between the discrete and continuum terms. The energies and J^π values for the discrete levels were taken from the adopted schemes of the Nuclear Data Sheets[31] supplemented by recent references[6,9,32] for ^{85}Rb, ^{93}Nb, and ^{98}Mo. I assigned uncertain and unknown J^π values consistently with neighboring levels.

The resulting $\langle\Gamma_\lambda\rangle_s$ for s-wave neutron resonances are shown by open symbols in Fig. 3(a). The circular experimental points are taken from the tabulation of Mughabghab and Garber[35] for those nuclei where at least four widths have been measured; the values are averages weighted by the quoted errors. The triangles are quoted averages from the recent work[10,12-16] for $88 \leq A \leq 100$. The experimental and calculated points are connected for each nucleus.

Figure 3(b) shows the ratio of experimental and calculated widths from Fig. 3(a). Two-thirds of the points lie within the limits, 1.0 ± 0.25, as indicated by the dashed lines. Basically this is a two-parameter fit which has been achieved using the curve from Fig. 1.

Two comments about the inadequacy of the experimental widths are appropriate. Firstly, the error bars on the solid circles represent only the errors in the weighted means and may not include much larger systematic errors. The bars on the triangles represent errors quoted by the authors and are generally larger than for the solid circles even though the triangles may be the more accurate.

Secondly, the data are not a complete sample of the nuclei in this mass region because the even targets are often omitted for lack of data. For example, the points from $A = 101$ to 109 include only odd targets. The model predicts odd-even effects. These are confirmed near $A = 98$. Also the relatively high values for the odd nuclei near $A = 105$ are consistent with the predictions; the even nuclei in this region are predicted to have

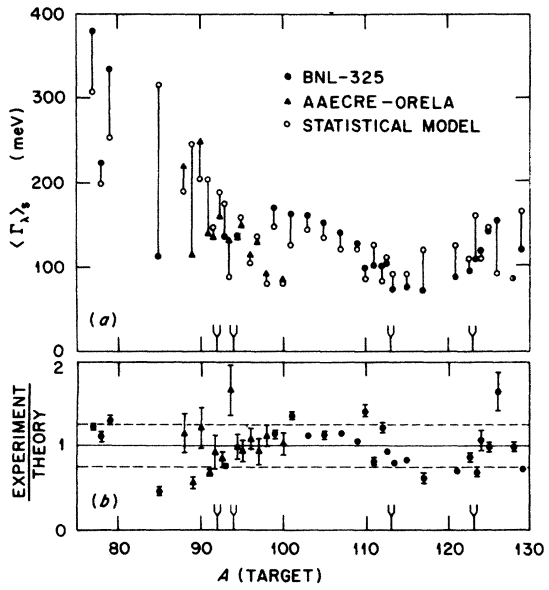

FIG. 3. (a) Predicted and observed radiation widths for s-wave neutron resonances. The AAECRE-ORELA data represent cooperative work from the Australian Atomic Energy Commission Research Establishment and the Oak Ridge Electron Linear Accelerator (Refs. 10 and 12–16). The BNL-325 points represent averages weighted inversely by the quoted variances from the tabulation in Ref. 35. The predictions are based in part on the strength functions from Sec. II and the density parameters from Table I and Fig. 2. For clarity experimental and theoretical symbols are connected. The two-pronged symbols on the abscissa show positions of isobaric pairs with the lower-Z plotted to the left. (b) Ratios of experimental to predicted widths from (a). The BNL-325 error bars represent errors of the weighted means and may not include large systematic errors. The AAECRE-ORELA errors were quoted by the authors. The dashed lines correspond to 1.0 ± 0.25.

lower values. However, the ^{110,111,112,113}Cd isotopes do not show the predicted odd-even effects. The origin of the odd-even effects is related to the nuclear temperatures discussed below.

V. DISCUSSION OF TEMPERATURES

The strength functions deduced above are intimately related to the level density function. This section elucidates the role of the densities. Since only ratios of densities enter into the spectrum in Γ_{cJ}, the important feature of $\rho_J(U)$ is its energy derivative. (The absolute value enters into the discrete term $\Gamma_{dJ\pi}$, which is important for certain A values as discussed in the next section.) The derivative is often expressed in terms of a nuclear temperature[28]:

$$1/T = d\ln[\rho(U)]/dU. \tag{15}$$

Although the foregoing analysis is based on the Fermi-gas model, for which T is energy-dependent, insight is gained from the constant temperature model

$$\rho(U) = C\exp(U/T). \tag{16}$$

If σ^2 is also constant, the Maxwellian-type spectrum of γ rays is approximately $E_\gamma^4\exp(-E_\gamma/T)$ and has its maximum near $E_\gamma = 4T$. Neglecting the discrete term we have approximately

$$\langle\Gamma_\gamma\rangle_J \approx 2.6\times10^{-7}(\sigma_g\Gamma_g^2/E_g^4)\int_0^\infty E_\gamma^4 e^{-E_\gamma/T}dE_\gamma$$
$$= 4!\times2.6\times10^{-7}T^5\sigma_g\Gamma_g^2/E_g^4. \tag{17}$$

This shows the essential role of the coefficient, $\sigma_g\Gamma_g^2/E_g^4$, which was plotted in Fig. 1; and it shows a T^5 dependence, which has its counterpart in the Fermi-gas model.

The Fermi-gas nuclear temperature is the inverse of $(a/U)^{1/2} - 3/2U$ but, since dipole radiation populates only states of spin J and $J\pm1$, a temperature T_J is of more interest. Let us define T_J by analogy with T:

$$1/T_J = d\ln[\rho_J(U)]/dU$$
$$= \left(\frac{a}{U}\right)^{1/2} - \frac{2}{U}\left[1 - \frac{(J-1/2)^2}{8\sigma^2}\right]. \tag{18}$$

We cannot give a simple approximation like Eq. (17) but we can illustrate the predictions using Eq. (17) if we compute T_J at some average excitation which lies below E_x but above the excitation corresponding to the mean of the γ-ray spectrum.

In Fig. 4 the solid curves were computed accu-

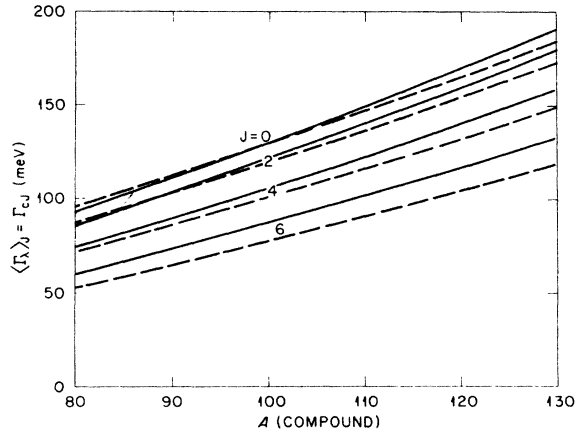

FIG. 4. Calculated radiation widths for average density parameters ($a = 13$ MeV^{-1} and $\Delta = 0$) with $E_x = 7.5$ MeV for N, Z, and A along the valley of β stability. The strength function parameters are from Eqs. (3)–(5) and (8). Solid curves were deduced by integration of the continuum width, Γ_{cJ}, and dashed curves were calculated approximately from effective temperatures.

rately by integration of Γ_{cJ} for fictitious nuclei with $E_x = 7.5$ and with N, Z in the valley of β stability. Each integration was extended to near the ground state. The parameters included the strength functions defined in Sec. II and average density parameters, $\Delta = 0$ and $a = 13$ MeV^{-1}. The dashed curves were then calculated approximately from Eq. (17) using values of T_J computed at 2.4 MeV below E_x. The widths are predicted to decrease with increasing J because the temperature decreases from about 0.83 MeV for $J = 0$ to 0.75 MeV for $J = 6$. The fact that the approximate dashed curves fall too rapidly shows that the effective energies for computing T_J should be increased for the higher J values. (The peak of the Maxwellian shifts to higher excitations.) For example, the curve for $J = 6$ would fit better if T_J were computed at only 2 MeV below E_x.

The A dependence for these curves results essentially from the $A^{4/3}$ variation in E_g^{-4} and is closely related to the curve in Fig. 1. For the actual nuclei analyzed in the preceding section this A dependence combines with the variation of nuclear temperature to give the variations in Γ_{cJ}.

The expression for T_J is complicated so that the dependence of Γ_{cJ} on E_x is not obvious. However, since Γ_{cJ} varies as T_J^5 and the leading term in T_J is proportional to $U^{1/2}$, we expect $\Gamma_{cJ} \propto U_x^{5/2}$. Detailed numerical integrations show this to be about right. In contrast, Γ_{cJ} for the constant temperature model is independent of E_x for a given nucleus, except for minor effects of the spin cutoff factor.

We see that the important feature of $\rho_J(U)$ is the effective temperature rather than the actual density. However, if the density is small its value is significant because it enters inversely into $\Gamma_{dJ\pi}$. This discrete term may then be large and, as discussed in the next section, a parity dependence is introduced because the discrete states are dominated by one parity and $E1 > M1$.

The Appendix gives further comments on the assumed density function.

VI. *P*-WAVE STATISTICAL ENHANCEMENTS

Boldeman *et al.*[12-15] and Musgrove *et al.*[10,16] found the experimental average radiation widths for p-wave neutron resonances to be larger than for s waves in the mass region $88 \leq A \leq 100$. The statistical contribution to $\langle\Gamma_\lambda\rangle_p - \langle\Gamma_\lambda\rangle_s$ is given by the difference in the discrete terms $\Gamma_{dJ\pi}$ for s- and p-wave resonances. Unlike the "continuum" width, which varies as T_J^5, this term varies directly with the average level spacing at E_x. Since the predicted spacings in Table I usually agree with those observed to within the large uncertainties of about ±25%, the foregoing calculations of p-s differences could be quoted at once. However, the philosophy of the present section is that the actual s-wave spacings should be used in predicting p-s differences. We could simply correct the observed spacings for spin dependences and then calculate the differences directly without bothering to adjust the gas constants or to repeat the "continuum." However, the following adjustments of the gas constants and repeat calculations are made to show that the strength functions are still consistent with the s-wave radiation widths.

TABLE II. Back-shifted Fermi-gas constants for $88 \leq A \leq 100$ to fit low-energy densities as well as the observed s-wave spacings from Table I.

Target	a (MeV^{-1})	Δ (MeV)
^{88}Sr	7.25	0.7
^{89}Y	10.16[a]	0.7[a]
^{90}Zr	8.10	0.1
^{91}Zr	9.64	1.6
^{92}Zr	10.33	0.6
^{92}Mo	9.61	0.8
^{93}Nb	11.44	−0.8
^{94}Zr	11.82	1.3
^{94}Mo	11.44	0.7
^{95}Mo	11.60	1.4
^{96}Mo	12.17	0.4
^{97}Mo	12.70	1.0
^{98}Mo	12.88	−0.1
^{100}Mo	13.20	−1.2

[a]Recent data by Camarda (Ref. 33) give a spacing of 4.0 keV for average 130-keV neutrons. For that spacing $a = 8.70$ MeV^{-1} and $\Delta = 0.3$ MeV in agreement with Fig. 2 and Table I.

Table II lists the values for a and Δ required to fit both the low-lying bound states and the s-wave resonant spacings for $88 \leq A \leq 100$ from Table I. The largest readjustment in a was for ^{89}Y. (As stated in the footnote, the ^{89}Y spacing recently found by Camarda[33] agrees with the prediction based on the smooth curve for a. Camarda's result, which became available after this analysis was complete, suggests that spacings predicted from a smooth curve may be as good as the experiments.)

Figure 5 compares the observed widths with the newly predicted $\langle\Gamma_\lambda\rangle_s$ for $88 \leq A \leq 100$. Some of the predictions differ from those in Fig. 3, particularly very near $A = 90$. Overall the predictions fit the data; the observed variations from nucleus to nucleus are generally confirmed.

The largest percentage deviation is for ^{94}Zr, which is predicted a factor of 2 too low. Perhaps the discrepancy could be due to experimentally unresolved resonances. To explore that possibility,

I deduced the triangular points for ^{94}Zr by averaging the experimental widths[13] in two groups. The lower triangle, which agrees with the prediction, is the average of eight resonances between 2 and 49 keV, and the upper triangle is the average of the remaining five resonances from 44 to 88 keV.

In Fig. 6 the solid bars are the predicted $\langle\Gamma_\lambda\rangle_p - \langle\Gamma_\lambda\rangle_s$. Having normalized to the observed s-wave spacings and having used strength functions which predict the "continuum" contribution quite well, we expect these differences to be fairly reliable. To these solid bars are added the valency predictions[1,2] which Boldeman *et al.*[12-15] and Musgrove *et al.*[10,16] calculated using observed reduced neutron widths and (d,p) spectroscopic factors. The summed bars generally agree with the experimental differences.[6,10,12-16] Indeed, the agreement is remarkable in light of the inherent uncertainties in the theory and in the differences of two large experimental numbers. Here as in Fig. 5, the largest discrepancy is for ^{94}Zr; and that is mostly removed as shown by the dashed bar by use of the lower triangle in Fig. 5.

It should be recognized that Fig. 6 is a plot of differences from the total radiative widths of Fig. 5 and that the fractional discrepancies between the observed and statistically predicted p-wave widths are relatively small. For the six nuclei from ^{88}Sr to ^{92}Mo, for example, the predicted p-wave widths average 85% of the observed. It seems possible that the experimental widths could be fit by extending the discrete states to higher energies.

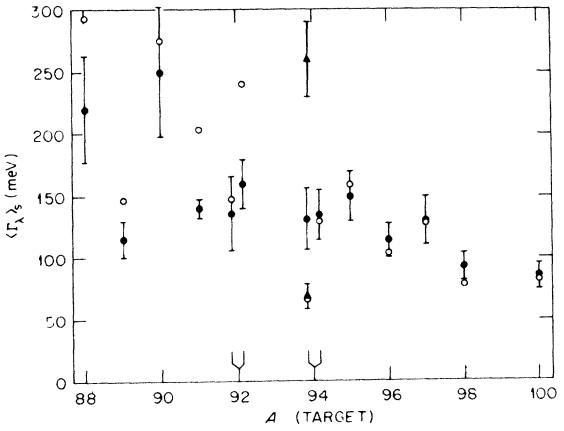

FIG. 5. Predicted and experimental radiation widths for s-wave resonances with fitted spacings. The solid circles show the AAECRE-ORELA data from Fig. 3. The predictions (open circles) are made as in Fig. 3 except that the Fermi-gas constants were adjusted (Table II) to fit the observed s-wave spacings. The two-pronged symbols are described in Fig. 3. The two triangles for ^{94}Zr were deduced by separating the observed widths (Ref. 13) into low- and high-energy groups.

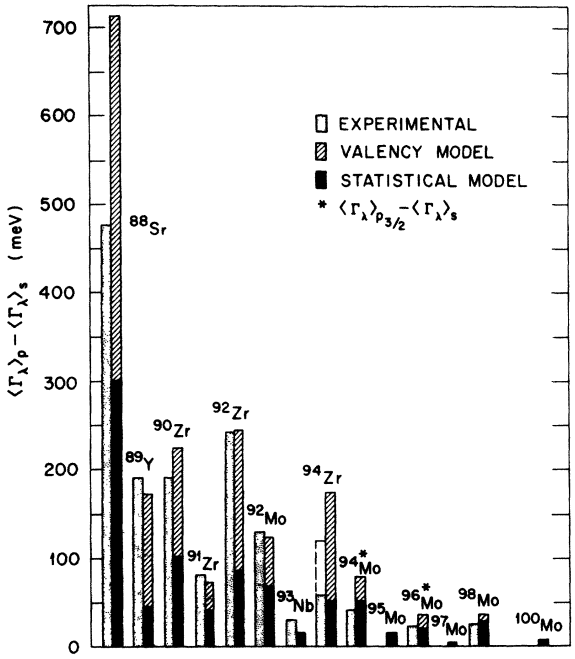

FIG. 6. Observed and predicted differences between p-wave and s-wave resonance widths. The s-wave widths (except ^{93}Nb) are from Fig. 5 and the p-wave widths can be deduced by summing values from both figures. The observed difference from ^{93}Nb was found by summing partial widths (Ref. 6). All other experimental values are from AAECRE-ORELA data on total widths (Refs. 10 and 12–16). For ^{94}Zr the higher experimental bar corresponds to the lower triangular point in Fig. 5. The valency predictions are also from Refs. 10 and 12–16 and the statistical predictions are from Sec. VI.

Thus, although Fig. 6 shows that the sum of valency and statistical contributions agrees well with the data, the mere fact that the statistical part by itself is too small would probably be insufficient evidence for a nonstatistical contribution.

These statistical p-s differences for $A \approx 90$ result from the large level spacings. For $100<A<130$ the differences are negligible. Below $A = 88$ there are predicted enhancements for s-wave resonances rather than p waves. The difference is 50% for ^{78}Se, however, that is based on the large predicted level spacing in Table I, which is a factor of 3 larger than the reported value.

VII. EXPERIMENTAL PARTIAL STRENGTHS AND WIDTHS

The strengths defined in Sec. II and used in Sec. IV and VI were designed essentially to describe total radiations to the many states at about half of the neutron separation energy. Certainly it could be that these strengths are quite wrong for the lower states either because the assumed Fermi-

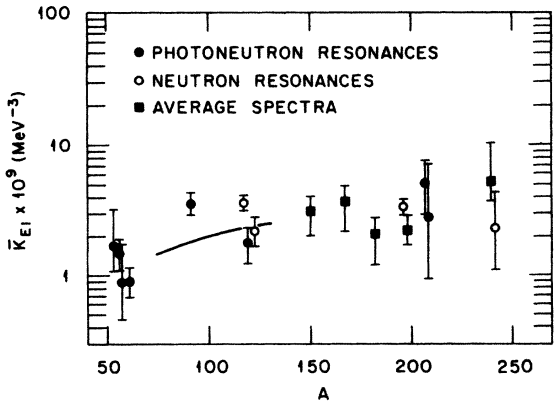

FIG. 7. Summary by Jackson (Ref. 36) of observed average $E1$ reduced widths for primary transitions to low-lying states. The ordinate is $\bar{k}_{E1} = S_{E1}(E_\gamma)A^{-2/3}$ where $S_{E1}(E_\gamma)$ is experimental for the points. The curve is calculated from the present evaluation of $S_{E1}(E_\gamma)$ for $E_\gamma = 7$ MeV and for nuclei along the valley of β stability for $75 < A < 130$.

gas temperatures are wrong or because the Axel-Brink hypothesis is invalid for the closely spaced high-lying states, or both. For example, if the assumed nuclear temperatures were systematically too high then the assumed strengths would have to be systematically too low in order to compensate for the T^5 term in Eq. (17). Such possible errors need to be examined by comparing the empirical strengths from Sec. II with those published for the low-lying states.

The data on strength functions are limited. Figure 7 shows Jackson's[36] recent summary of strengths, expressed as the usual reduced width $\bar{k}_{E1}$ and deduced from data on average capture spectra, resonance capture spectra, and threshold photoneutron spectra. The ordinate is given by a standard definition[36] and is the same as

$$\bar{k}_{E1} = S_{E1}(E_\gamma)A^{-2/3}, \tag{19}$$

where $S_{E1}(E_\gamma)$ is an experimental strength defined by Eq. (1) for transitions to a given low-lying state. The points include only data which average over a sufficient number of excited states at E_x in order to suppress the statistical effects of Porter-Thomas fluctuations.

The line for $75 < A < 130$ is calculated from the present $S_{E1}(E_\gamma)$ for $E_\gamma = 7$ MeV for nuclei along the valley of β stability. The A dependence for this curve is essentially $A^{2/3}$ and comes from the $A^{4/3}$ term in the approximation of Eq. (7). The good agreement of the curve with the data supports the present use of the Axel-Brink hypothesis and the Fermi-gas temperatures for the "continuum" states.

Since the predicted radiation widths vary directly with the strength functions, any new information that might become available and force a significant renormalization of the strengths would also force the Axel-Brink hypothesis or the Fermi-gas model to be modified in order to retain the average fits to the observed total widths.

No attempt is made here to compare in detail the predicted and observed partial widths for specific final states. However, the ground state transition width for $p_{3/2}$ resonances in $^{90}\mathrm{Zr}(n,\gamma)^{91}\mathrm{Zr}$ is of particular interest because Toohey and Jackson[17] made detailed measurements on the inverse reaction. They found an average partial width of 149 eV, of which roughly 87 eV was calculated to be valency. The predicted width from the preceding section is 69 eV or about equal to the nonvalency part (149 – 87 = 62 eV). Both experiment and theory have uncertainties; nevertheless, this agreement shows that the observed excess over the valency contribution can be attributed to statistical processes, contrary to the conclusion of Boldeman *et al.*[12] that the excess is too large to be statistical.

VIII. CONCLUSIONS

For $75 < A < 130$ the statistical model can be reasonably parametrized to describe most of the average radiation widths. The average widths for s-wave resonances are fitted to a standard deviation of about ±25% on the basis of the Axel-Brink hypothesis using the back-shifted Fermi-gas model for level densities with parameters chosen to fit known densities. In general the predictions are as good as the experiments, which suffer from limited sample size and systematic uncertainties. Odd-even effects are predicted and are partially confirmed by recent data for $A \approx 98$. The fit is achieved by adjusting two free parameters to give the magnitude and A dependence for the low-energy tail of the giant dipole resonance. The resulting strength functions from this application of the Axel-Brink hypothesis and the Fermi-gas model to relatively high-lying states are consistent with those observed for transitions to the lower states.

The statistical model is often used to predict average neutron-capture cross sections. In that formalism each term related to γ rays is usually expressed as the ratio $\langle\Gamma_\lambda\rangle/\langle D\rangle$ of average total radiation widths to level spacing because, expressed in that form, the γ-ray factors appear in a manner parallel to the neutron transmission factors. Actually, $\langle\Gamma_\lambda\rangle$ is not closely related to $\langle D\rangle$ but, rather, depends on the rate of change of $\langle D\rangle$ or on the nuclear temperature. The width varies with the fifth power of an effective temperature. The resulting dependence of $\langle\Gamma_\lambda\rangle$ on mass and excitation

energy is rather weak, in sharp contrast to the strong dependence for $\langle D\rangle$.

However, for the partial width to a given final state the ratio $\langle\Gamma_{\lambda f}\rangle/\langle D\rangle$ or partial width per energy interval is of fundamental physical significance. Generally the level densities at neutron binding are so high that relatively little partial width is available for any particular final state. But near the 50-neutron shell at $A\approx 90$, densities are small enough such that a relatively large fraction of transitions go to the low states, which are mostly even parity. Thus, for the even parity targets near $A=90$ there is considerable enhancement in radiation widths predicted for p-wave neutron resonances relative to s waves. [For ^{89}Y(n,γ) the p-wave states are even parity and the low-lying low-spin states are mostly odd parity.] Experimentally p-s differences have been found near $A=90$. Valency components have been identified in the literature by the correlation of neutron, (d,p), and radiation widths; and these components added to the statistical components presented here give a good description of the observed p-s differences. On average the predicted valency and statistical contributions to p-s differences are about equal.

ACKNOWLEDGMENTS

I am grateful to Dr. J. L. Fowler, Dr. J. A. Harvey, Dr. D. J. Horen, Dr. R. L. Macklin, Dr. S. K. Penny, Dr. S. Raman, and Dr. R. R. Winters for stimulating discussions. I am particularly indebted to Dr. Penny for use of his computer program.

APPENDIX

We can question whether or not the Fermi-gas model provides us with a good estimate of the effective temperature. Fitting the model to two data "points", one near the ground state and the other at the neutron separation energy, does not guarantee correct temperatures in the intermediate region. In principle, intermediate temperatures can be measured for stable nuclei and certain unstable nuclei (usually not those from neutron capture) by observing the boil-off spectrum for (n,n') and (p,n) reactions. Many such spectra have been observed[26] and the (n,n') work of Maruyama[37] is often quoted. For the present mass region Maruyama found the elements Nb, Ag, Sb, and I to have temperatures increasing with excitation energies consistently with a Fermi-gas, whereas Sr, Y, and Sn (nuclei near the 50-nucleon shells) had temperatures increasing more slowly. For Sr the temperature was nearly constant.

However, the actual temperatures deduced by Maruyama for stable nuclei are about 0.2 to 0.3 MeV less than those deduced here. Therefore, they are inconsistent with the ratios of the s-wave resonant spacings to the spacings of all levels near the ground states for the neighboring neutron-capture nuclei. This discrepancy in temperature corresponds roughly to a factor of 50 in the ratio of s-wave spacings to the spacings near ground. The reason for the discrepancy is not clear. It would be reduced if there were many more s-wave resonances than observed and if these represented a smaller fraction of the total density than predicted by the spin factor. It seems unlikely that such errors would account for all of the discrepancy. There can also be serious errors in interpreting (n,n') boil-off spectra, as emphasized by Huizenga and Moretto.[26]

One might conclude from Maruyama's work that a model with constant temperature should be substituted near $A=90$ and 120 (near the 50-nucleon shells) with parameters chosen to fit the two density data "points." Naively, we might anticipate this change to allow the strength functions to follow more closely the pattern of GDR data points in Fig. 1, with relatively lower values near the 50-nucleon shells. Actually, the effect is in the opposite direction; the strengths would have to be increased near the shells because the width varies as T^5 and the constant T would be smaller than for a Fermi gas. On the other hand, the comparisons of predicted and observed widths in Fig. 3 suggest that either T or $S(E_\gamma)$ should be reduced near $A=120$. The use of a constant-temperature model with the same strength functions would reduce the predicted widths a factor of 2 near $A=120$ and about 20% or less near $A=90$. The use of a constant temperature model for all A values would require larger strength functions to restore the average agreement with the widths.

Bartholomew *et al.*[18] used constant temperatures in their review of strength functions. My conclusion is that the back-shifted Fermi-gas model has both experimental and theoretical support[26] and is the best simple model for this mass region.

---

*Research sponsored by U. S. Energy Research and Development Administration under contract with Union Carbide Corporation.

[1]A. M. Lane and J. E. Lynn, Nucl. Phys. 17, 586 (1960).

[2]J. E. Lynn, *Theory of Neutron Resonance Reactions* (Clarendon, Oxford, England, 1968), Chap. VII.

[3]A. M. Lane, Phys. Lett. 31B, 344 (1970); Ann. Phys. (N.Y.) 63, 171 (1971).

[4]M. Beer, Ann. Phys. (N.Y.) 65, 181 (1971).
[5]K. Ramawi, R. E. Chrien, J. B. Garg, M. R. Bhat, D. I. Garber, and O. A. Wasson, Phys. Rev. Lett. 23, 1041 (1969).
[6]R. E. Chrien, K. Rimawi, and J. B. Garg, Phys. Rev. C 3, 2054 (1971).
[7]G. Rohr, H. Weigmann, and J. Winter, Nucl. Phys. A150, 97 (1970).
[8]S. F. Mughabghab, R. E. Chrien, O. A. Wasson, G. W. Cole, and M. R. Bhat, Phys. Rev. Lett. 26, 1118 (1971).
[9]R. E. Chrien, G. W. Cole, G. G. Slaughter, and J. A. Harvey, Phys. Rev. C 13, 578 (1976).
[10]A. R. de L. Musgrove, B. J. Allen, J. W. Boldeman, and R. L. Macklin, Nucl. Phys. A270, 108 (1976).
[11]O. A. Wasson and G. G. Slaughter, Phys. Rev. C 8, 297 (1973).
[12]J. W. Boldeman, B. J. Allen, A. R. de L. Musgrove, and R. L. Macklin, Nucl. Phys. A246, 1 (1975).
[13]J. W. Boldeman, A. R. de L. Musgrove, B. J. Allen, J. A. Harvey, and R. L. Macklin, Nucl. Phys. A269, 31 (1976).
[14]J. W. Boldeman, B. J. Allen, A. R. de L. Musgrove, R. L. Macklin, and R. R. Winters, Nucl. Phys. A269, 397 (1976).
[15]J. W. Boldeman, B. J. Allen, A. R. de L. Musgrove, and R. L. Macklin, Nucl. Sci. and Eng. (to be published).
[16]A. R. de L. Musgrove, J. W. Boldeman, B. J. Allen, J. A. Harvey, and R. L. Macklin (unpublished).
[17]R. E. Toohey and H. E. Jackson, Phys. Rev. C 9, 346 (1974).
[18]G. A. Bartholomew, E. D. Earle, A. J. Ferguson, J. W. Knowles, and M. A. Lone, in *Advances in Nuclear Physics*, edited by M. Baranger and E. Vogt (Plenum, New York, 1973), Vol. 7, p. 229.
[19]D. M. Brink, Ph.D. thesis, Oxford University, Oxford, England, 1955 (unpublished).
[20]P. Axel, Phys. Rev. 126, 671 (1962).
[21]N. Rosenzweig, Nucl. Phys. A118, 650 (1968).
[22]B. L. Berman, At. Data Nucl. Data Tables 15, 319 (1975).
[23]J. S. Levinger, *Nuclear Photo-Disintegration* (Oxford U. P., London, 1960).
[24]L. M. Bollinger, in *Proceedings of the International Conference on Photonuclear Reactions and Applications, Asilomar*, 1973, edited by B. L. Berman (Lawrence Livermore Laboratory, Univ. of California, 1973), CONF-730301, p. 783.
[25]L. M. Bollinger, and G. E. Thomas, Phys. Rev. C 2, 1951 (1970).
[26]J. R. Huizenga and L. G. Moretto, Annu. Rev. Nucl. Sci. 22, 427 (1972).
[27]E. Gadioli and L. Zetta, Phys. Rev. 167, 1016 (1968).
[28]A. Gilbert and A. G. W. Cameron, Can. J. Phys. 43, 1446 (1965).
[29]W. Dilg, W. Schantl, H. Vonach, and M. Uhl, Nucl. Phys. A217, 269 (1973).
[30]J. A. Holmes, S. E. Woosley, W. A. Fowler, and B. A. Zimmerman, At. Data Nucl. Data Tables 18, 305 (1976).
[31]Nuclear Data Group, Data Sheets, Volumes 5–19.
[32]J. E. Holden, J. J. Kolata, and W. W. Daehnick, Phys. Rev. C 6, 1305 (1972).
[33]H. S. Camarda, Bull. Am. Phys. Soc. 22, 631 (1977); and (private communication).
[34]S. K. Penny, Computer Science Division at Oak Ridge National Laboratory, private communication.
[35]*Resonance Parameters*, compiled by S. F. Mughabghab and D. I. Garber, Brookhaven National Laboratory Report No. 325 (National Technical Information Service, Springfield, Virginia, 1973) 3rd ed., Vol. 1.
[36]H. E. Jackson, in *Proceedings of the Second International Symposium on Neutron Capture Gamma-Ray Spectroscopy* (Reactor Centrum Nederland, Petten, The Netherlands, 1975), p. 437.
[37]M. Maruyama, Nucl. Phys. A131, 145 (1969).

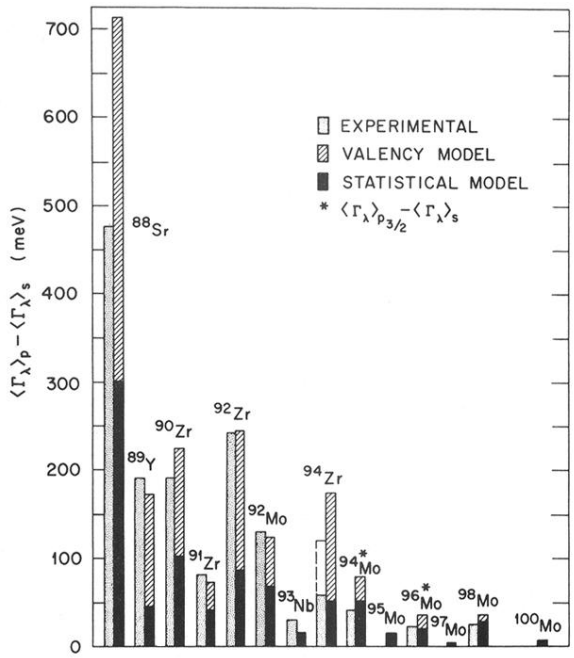

FIG. 6. Observed and predicted differences between p-wave and s-wave resonance widths. The s-wave widths (except ^{93}Nb) are from Fig. 5 and the p-wave widths can be deduced by summing values from both figures. The observed difference from ^{93}Nb was found by summing partial widths (Ref. 6). All other experimental values are from AAECRE-ORELA data on total widths (Refs. 10 and 12–16). For ^{94}Zr the higher experimental bar corresponds to the lower triangular point in Fig. 5. The valency predictions are also from Refs. 10 and 12–16 and the statistical predictions are from Sec. VI.